



Virtualized resource sharing in cloud radio access networks: An auction approach



Ruiting Zhou^{*,a}, Xunrui Yin^b, Zongpeng Li^c, Chuan Wu^d

^a University of Calgary, Calgary, AB, Canada

^b SKLSE, School of Computer, Wuhan University, China

^c SKLSE, School of Computer, Wuhan University and the University of Calgary, Calgary, AB, Canada

^d University of Hong Kong, Kowloon, Hong Kong

ARTICLE INFO

Keywords:

Cloud radio access networks (C-RAN)
Network function virtualization (NFV)
Mechanism design

ABSTRACT

As mobile terminals proliferate and mobile Internet traffic explodes, demand for efficient and high capacity cellular access escalates. Two fundamental techniques are being implemented to help meet such a demand. The first is virtualization based, centralized cloud processing. Baseband signals are sampled and transmitted through front-haul links to a mobile cloud, for processing by mobile base station instances deployed in an on-demand fashion. User and channel information are aggregated to the cloud, facilitating optimized decision making. The second is the separation of infrastructure ownership from service provisioning in cellular networks. The “Tower” company now specializes in deployment and maintenance of the cloud-radio access network (C-RAN) infrastructure. Mobile operators focus instead on their sole business of wireless service provisioning. Mobile operators lease C-RAN resources that include spectrum resources at remote radio heads, front-haul bandwidth and mobile base station instances. This work proposes a natural auction approach for inter-operator resource sharing, where each operator bids a capacitated sub-network of the C-RAN. Drawing from the theories of Maximal-in-Range auctions and efficient graph algorithms, we design and test a C-RAN resource auction that is truthful, polynomial-time computable, and achieves close-to-optimal social welfare.

1. Introduction

As mobile devices and applications proliferate and mobile access to the Internet grows, demand on capacity and efficiency of cellular networks escalates. The transition from 4G (LTE and LTE-Advanced) to 5G cellular technologies in the upcoming years aims to provide substantially enhanced system capacity and data transmission efficiency through a number of new technologies that include cloud computing based radio access networks (C-RAN) and network function virtualization (NFV) [30]. The fundamentally new technologies in future cellular networks demand new resource management algorithms and protocols that work in concert with infrastructure and hardware changes. This work draws the community’s attention to the problem of virtualized resource sharing among mobile operators in a C-RAN, and designs and tests auction based solutions.

An important infrastructure revolution in cellular networks is the deployment of C-RAN, for cloud computing based, centralized information processing and system optimization. A traditional base station (BS) includes a complex signal processing unit, for A/D D/A conversion [31]. The processing capacity of the BS needs to be large

enough even in peak hours. However, traffic volume at a BS fluctuates dramatically across the temporal domain, and peak traffic volume may be substantially higher than average. As a result, the utilization of an individual BS is rather low. As inter-BS sharing of processing resources is infeasible in the traditional cellular infrastructure, considerable processing capacity and energy are wasted. The cloud radio access network (C-RAN) is a new cellular network infrastructure based on cloud computing and NFV [32]. Remote Radio Heads (RRHs) at BSs are to be greatly simplified, with functions pushed toward mobile clouds (data centres) that each manages a group of BSs. Analog signals from RRHs are sampled, quantized, and transmitted through a front-haul network to the cloud. The cloud hosts a pool of virtual BS instances for processing baseband signals with functions such as channel coding and modulation. Virtual BS instances are provisioned in an elastic fashion, following realtime demand from RRHs. Centralized information and processing in the C-RAN further facilitates system-wide optimization and cost-saving, such as centralized management, cooperative communication and joint decoding [21].

Another important trend in cellular networks is service-infrastructure separation, *i.e.*, the separation of infrastructure ownership

* Corresponding author.

E-mail addresses: rzho@ucalgary.ca (R. Zhou), xunyin@ucalgary.ca (X. Yin), zongpeng@ucalgary.ca (Z. Li), cwu@cs.hku.hk (C. Wu).

from cellular service provisioning. Constructing and operating BSs represents a major expense of traditional mobile operators. For example, carriers in China spent more than \$200 billion US to maintain and build BSs from 2008 to 2012, but the utilization rate of the processing resources and fibre-optic links is only 1/3 [2]. The creation of the “Tower” company was recently witnessed in a few markets around the world since 2013 [3]. In China, a national Tower company was created in July 2014, taking over BSs from three major mobile operators [3]. The Tower company is responsible for designing, building and maintaining BSs. It further operates regional data centres that manage BSs and process baseband signals. In the US, AT&T sold their BS subsystem in October 2013 to Crown Castle, currently the largest provider of shared cellular infrastructure in the US with approximately 40,000 BS towers [1]. The vision of 5G and beyond is that the Tower company is dedicated to the deployment and ownership of the C-RAN infrastructure. Mobile operators are freed from infrastructure maintenance, and focus explicitly on their core business of providing the best mobile Internet service. Using virtualization technologies, mobile operators lease resources (spectrum resources at BSs, virtual BS instances and front-haul bandwidth) from the Tower company to serve their customers.

Similar to the cloud computing market where long term contracts and short term auctions complement each other for meeting customers’ need of virtual machine instances, mobile operators are expected to sign long term contracts for baseline service coverage, and acquire additional resources in short term through auctions to cover temporal and spatial demand spikes. This work proposes an auction based market mechanism for such short-term C-RAN resource leasing. Such a C-RAN auction has a salient feature that separates itself from wireless spectrum auctions [12] and virtual machine auctions [26] that have been extensively studied — the bid of each mobile operator is naturally expressed as a sub-network of the C-RAN, and the C-RAN faces a sub-network packing problem in social welfare maximization. We study the C-RAN resources auction under two front-haul models: point-to-point, *i.e.*, every BS has its own fibre to the cloud, and daisy chain, *i.e.*, BS share fibre links to the cloud in groups.

The underlying sub-network packing structure renders the C-RAN auction NP-hard, even if truthful bids are given for free. The key techniques we employ for designing an efficient and truthful auction include (a) exploiting the planarity of the C-RAN topology, and (b) Maximum-in-Range (MIR) auction theory. **First**, we design an exact algorithm to maximize social welfare over a given solution space of feasible C-RAN resource allocation. The time complexity of the exact algorithm is highly dependent on the structure of the feasible solution space to which it is applied, and is exponential over the entire feasible solution set. **Second**, our auction pre-commits to a set of carefully chosen solutions of social welfare maximization problem, such that (a) the chosen set is well-structured and allows polynomial-time maximization of the social welfare using the exact algorithm, and (b) the set is sufficiently large and effective, so the optimal solution inside this set approaches global maximum sufficiently closely. An alternative view to the second step is that the exact algorithm together with the pre-commitment step constitutes an approximation scheme to the C-RAN welfare maximization problem. **Third**, we adapt VCG-style payments to work in concert with the exact algorithm and the pre-commitment step, and show that the auction is truthful. The end result is a C-RAN resource auction that is truthful, polynomial-time computable, and guarantees $(1 - \epsilon)$ economic efficiency. We next provide a more detailed overview of the key steps.

We formulate the C-RAN social welfare maximization problem as an integer linear programming problem, which is proven to be NP-hard even for a constant number of BSs or a constant number of mobile operators. We first design an exact algorithm for computing an optimal allocation among a given feasible solution set. The exact algorithm exploits the unique planar topology of a C-RAN, and combines dynamic programming and planar graph bisection techniques in an algorithm

that is as computationally efficient as possible, while guaranteeing output optimality. The running time of the exact algorithm is exponential on the original solution space, and is proven to be polynomial on the well-structured subspace of solutions that we pre-commit to.

Given the exact algorithm, an obvious solution is to apply it together with the VCG auction framework to obtain a truthful C-RAN auction. However, such a VCG auction can handle only very small C-RAN topologies. Empirical results show that the computation time of the VCG auction for a C-RAN system with a few layers of BSs already exceeds one minute. A key step in our C-RAN auction design is to utilize the exact algorithm on a well-structured subspace of solutions, obtaining a much more efficient approximation scheme. Our empirical studies suggest that our C-RAN auction algorithm can handle a C-RAN topology consisting of thousands of base stations in seconds. The idea in our approximation scheme design (solution subspace selection) is based on the observation that the running time of the exact algorithm is exponential to the parameter k , for a C-RAN topology that is k -outerplanar (k layers of BS cells). Instead of working directly on a k -outerplanar C-RAN, the auction examines instead a sequences of dissected outerplanar graphs, each with a series of k' -outerplanar components, where k' is a constant smaller than k . Our approximation scheme is parameterized by a tunable constant ϵ , based on which we can tradeoff between solution optimality and computational complexity.

Given the approximation scheme, our final step towards the C-RAN auction design is to apply the MIR auction design technique that has recently witnessed a number of successful applications [4,22]. We take a retrospect on the approximation scheme, verify that it effectively pre-commits to a well-structured subset of feasible solutions. The approximation ratio analysis provides a guarantee that the optimal solution in the subset is indeed close to the optimal solution in the entire feasible solution set. The approximation scheme can therefore be combined with a VCG-style payment mechanism to become an MIR auction, which is efficient, elicits truthful bids for C-RAN resources from mobile operators, and guarantees close-to-optimal social welfare.

To verify the efficacy of the proposed C-RAN auctions for inter-operator resource sharing, we have conducted extensive real-world trace-driven simulation studies, verifying the time efficiency, the social welfare performance, and details in the resulting resource allocation in both point-to-point and daisy chain front-haul models. Simulation results for large scale C-RAN systems show that the proposed auctions can handle C-RAN graphs with up to thousands of BSs; the resource allocation from the auction achieves about 99% of maximum social welfare. That suggests in real world systems, the performance of the auction algorithm can be much better than the guaranteed approximation ratio, which corresponds to the theoretical worst case.

In the rest of the paper, we review background and related work in Section 2, and describe the C-RAN system model in Section 3. Sections 4 and 5 present the auction schemes for C-RANs with point-to-point front-hauls and daisy chain front-hauls, respectively. Section 6 presents performance evaluation. Section 7 concludes the paper.

2. Background and related work

Resources for lease through the C-RAN auction include spectrum resources, virtual BS instances and front-haul bandwidth. Although existing studies abound on spectrum auctions [10,12] and cloud resource auctions [34,37], this work is the first that tailors a truthful auction for the C-RAN system to allocate all three types of resources, which has a unique sub-network packing structure.

We briefly overview the background on C-RAN spectrum resources. Current mobile networks support both frequency-division duplex (FDD) and time-division duplex (TDD) modes [16]. FDD splits the channel frequency into many small *subcarriers* spaced at 15kHz, and then modulates each individual subcarriers using a digital modulation scheme (*e.g.*, 64-QAM). TDD splits a subcarrier into alternating time periods for downlink and uplink transmission. In future mobile

networks that use spectrum bands up to 60 GHz [39], a unit of spectrum resource may consist of hundreds of continuous subcarriers, and the number of available spectrum resources in each BS is limited by its channel bandwidth.

We next review related literature and background of the C-RAN system. A regional C-RAN includes three components: (i) base stations, (ii) a mobile cloud (data centre), and (iii) the front-haul network.

Base stations: BSs equipped with RRHs are used to transmit/receive signals to/from user equipments (UEs). Signal processing functionalities, while traditionally located on BSs, are virtualized and run remotely as mobile BS instances in the cloud data centre. The main technical challenge on BSs becomes making RRHs power-efficient and scalable [5,7].

Front-haul: The C-RAN front-haul transmits signals between BSs and the cloud, usually through a fibre network. The front-haul is a capacity bottleneck of the C-RAN, since bandwidth requirement is significantly higher for transmitting baseband sampling data [9]. The front-haul can have either a point-to-point topology or a daisy chain topology [9,21]. In a point-to-point C-RAN, each BS is connected directly to the cloud. When bandwidth requirement for baseband signal transmission rises to dozens of Gbps in the future mobile networks, this solution could be expensive as demand for the number of fibres per BS increases quickly. In a daisy chain C-RAN, through wavelength-division multiplexing (WDM), neighbour BSs are connected to a multiplexer/demultiplexer, and share optical links to the cloud. Besides physical implementation of the front-haul, some researchers investigate the transmission scheme in the front-haul. Sundaresan et al. [28] propose an intelligent configuration of the front-haul that deploys appropriate transmission strategies to maximize the traffic demand satisfied on the RAN.

The mobile cloud: The mobile cloud hosts and allocates a pool of virtual BS instances. A virtual BS instance is a virtual machine that specializes in signal processing functionalities (PHY, MAC, and network layer) traditionally found at BSs. Zhu et al. [40] introduce the steps of building a virtual BS pool and implement the first working prototype on a multi-core IT platform. Other studies focus on the design of resource allocation in the cloud data centre. Bhaumik et al. [8] analyse real-world trace data and show that the use of homogeneous computing resources for processing signals from BSs has the potential to save computing resources. Pompili et al. [24] present novel reconfigurable solutions for provisioning and allocation of virtual BSs, and discuss their pros and cons. Tang et al. [29] investigate a cross-layer resource allocation problem for C-RAN to minimize the overall system power consumption.

Auction mechanisms for cloud resource sharing have been extensively studied. Zhang et al. [35] apply a decomposition technique to design a randomized combinatorial auction for dynamic cloud resource provisioning. Sun et al. [27] propose a Nash equilibrium based cloud resource allocation algorithm by using a double auction method. However, they provide no proven guarantee for the approximation ratio in social welfare. Zhang et al. [36] aim to maximize total revenue while minimizing the energy cost for the cloud resource allocation problem. Different from the above literature, this work focuses on the allocation of C-RAN resources to mobile operators, targeting social welfare maximization. We propose a truthful auction for the operators to lease three types of virtualized resources from a tower company. The design of the auction applies algorithmic methods for manipulating a type of graphs known as k -outerplanar graphs, which naturally characterizes the cellular topology found in a C-RAN.

Along the direction of mechanism design for C-RAN resource sharing, Zhu et al. [38] design a combinatorial auction mechanism to jointly address the hierarchical resource allocation problem in 5G networks. Gu et al. [14] propose the first online auction to jointly allocate C-RAN resources. They assume bidders arrive online and bid for current resources. The above literature ignore the role of links that connect neighbour BSs. Moreover, our mechanism achieves

$(1 - \epsilon)$ -optimal social welfare, which significantly outperforms other mechanisms.

Our C-RAN auction design was partly inspired by a general technique of Baker [6] for designing approximation algorithms over k -outerplanar graphs. They propose a decomposition technique to work on k -outerplanar graphs. When applied to the maximum independent set problem, their algorithm guarantees $(k/k + 1)$ -approximation. Besides such k -outerplanar graph partitioning, our C-RAN auction design further requires an entirely different algorithm for processing the partitioned sub-graphs and MIR auction theory for converting approximation algorithms into truthful auctions.

3. System model and preliminaries

We consider a cloud radio access network (C-RAN) in a geographical region where M BSs are connected to a cloud data centre via optical fibre links (front-haul). Each BS hosts RRHs that transmit and receive signals. The signal processing units of the BSs are virtualized into virtual BS instances and are moved from the cell site into the cloud data centre, for resource consolidation and virtualization. The data centre maintains a virtual BS instance pool, and allocates virtual BS instances and each base station's spectrum resources. Mobile network operators lease resources for data transmissions from a Tower company that owns the C-RAN infrastructure. They sign a long-term contract (e.g., six months) with the Tower company for covering a baseline demand. Short-term leases of additional resources are conducted through auctions, for meeting transient demand hikes (e.g., half an hour). We consider the short-term C-RAN resource auction in two representative C-RAN models: point-to-point front-haul and daisy chain front-haul.

We consider the general case where the mobile operator bids for not only resources at the BSs but also links between certain BS pairs. Such inter-BS links play an important role in C-RAN control and optimization. For example, Coordinated multipoint (CoMP) is a promising technology in LTE and 5G to reduce the interference and improve the transmission data rate, which is a main element on the LTE roadmap beyond Release 9 [18]. Neighbour BSs coordinate in communication session by sharing data and information such as channel state information [17]. It is natural and practical to consider direct communication links, either fibre or wireless, between neighbour BSs [19]. Control messages such as handover messages can also be transmitted in a timely fashion via such inter-BS links.

3.1. C-RAN with point-to-point front-haul

Fig. 1 illustrates a C-RAN with point-to-point front-haul where each BS is connected directly to the cloud [15]. Let $[N]$ be the set of numbered mobile operators $\{1, 2, \dots, N\}$ with cardinality N . A C-RAN is modelled by a node-capacitated graph $G = (\mathcal{M}, \mathcal{E})$. Each node $m \in \mathcal{M}$ ($|\mathcal{M}| = M$) is an abstraction of the spectrum resources at BS m in the cloud, and front-haul links between BS m and the cloud. \mathcal{E} is the set of links between BSs. Direct communication between BSs has rather low data rate, hence we assume no capacity limits on links in \mathcal{E} .

Assume that one virtual BS instance controls a unit spectrum resource and the data generated by a spectrum resource is 1 unit per second. Let R_m denote the available amount of spectrum resource in

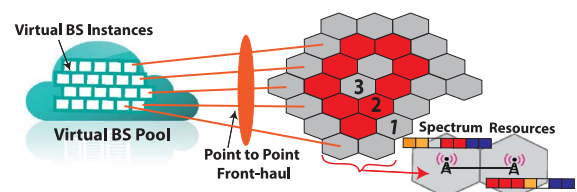


Fig. 1. C-RAN with point-to-point front-haul.

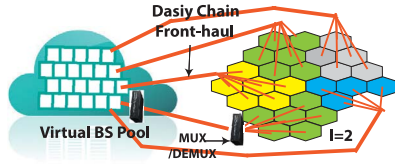


Fig. 2. C-RAN with daisy chain front-haul.

base station m . We relax the capacity limit for the number of virtual BS instances in the cloud, under the assumption that the C-RAN capacity bottleneck lies in the front-haul and the BSs [9,25]. With point-to-point front-haul, inter-BS front-haul capacity competition is non-existent, and we further assume that the bottleneck lies at the network of BSs.

3.2. C-RAN with daisy chain front-haul

Fig. 2 shows a C-RAN with daisy chain front-haul [15]. Let g denote a transmission group in the C-RAN system where several BSs share optical links to the cloud. We assume that the maximum number of hops between two BSs in a group is limited by a threshold l . In Fig. 2, up to six base stations are cascaded towards the cloud ($l = 2$). This model results in inter-BS competition of front-haul capacity. Let C_g denote the capacity (in units per second) of the shared optical links of group g .

3.3. The C-RAN resource auction

During each round of the C-RAN auction, an operator who predicts a resource shortage submits to the cloud a bid that corresponds to a capacitated subnetwork of the C-RAN graph. The bid submitted by operator n is of the format $(r_{n,m}, w_{n,m}, c_{n,e})$. Here $r_{n,m}$ is the number of unit spectrum resources requested at BS m , which implies an equal number of virtual VM instances and an equal number of front-haul link capacity units. $w_{n,m}$ is the willingness to pay for the resources at node m . If an operator n receives two adjacent BS nodes m_1 and m_2 , then further having access to the link e between m_1 and m_2 results in an extra gain from link e , owing to the benefit of CoMP. Let $c_{n,e}$ denote the average MIMO multiplexing gain and average diversity gain that operator n received from link e .

The cloud may accept either the bid subgraph in its entirety, or an induced sub-graph of the bid subgraph. The mobile operator n is willing to pay the summation of node utilities $w_{n,m}$ over all node m plus the summation of link utilities $c_{n,e}$ over all links e in the accepted sub-graph. The cloud solves a subgraph packing problem to decide the resource allocation S , and compute the payments for winning operators. S includes two types of binary number: $x_{n,m}$ is 1 if operator n successfully receives resources at BS m , and 0 otherwise; $y_{n,e}$ is 1 if operator n obtains link e , and 0 otherwise. The accepted sub-graphs packed together have to respect node capacities in the original C-RAN graph. Let p_n be the payment of operator n , $\forall n \in [N]$. Table 1 lists notation for ease

Table 1
Summary of notations.

N	# of operators	$[N]$	integer set $\{1, \dots, N\}$
M	# of base stations	p_n	payment of operator n
$V(S)$	social welfare achieved by the allocation S		
G	$G = (\mathcal{N}, \mathcal{E})$, the C-RAN graph		
$r_{n,m}$	amount of requested resources by operator n at BS m		
$w_{n,m}$	bidding price of $r_{n,m}$ resources in operator n 's bid		
$c_{n,e}$	bidding price of link e in operator n 's bid		
$w'_{n,m}$	valuation of $r_{n,m}$ resources in operator n 's bid		
$c'_{n,e}$	valuation of link e in operator n 's bid		
$x_{n,m}$	operator n receives resource at BS m (1) or not (0)		
$y_{n,e}$	operator n bids link e successfully (1) or not (0)		
R_m	available spectrum resources at base station m		
C_g	capacity of shared fibre for transmission group g		

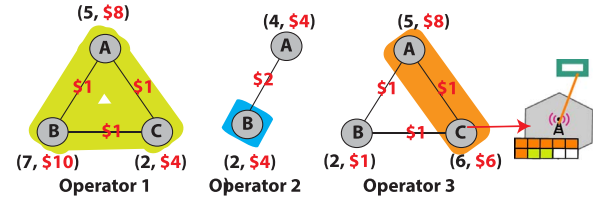


Fig. 3. Operators bid subnetworks of the C-RAN.

of reference.

Fig. 3 shows a simple C-RAN graph with 3 BSs. Assume three operators submit bids. Each BS is labelled with the amount of desired resources and valuation, and each inter-BS link is labelled with its valuation. The amount of available spectrum resources at each BS is 10. Each operator's bid subgraph is shown in the figure. The optimal resource allocation is highlighted in each operator's bidding subnetwork.

Let $w'_{n,m}$ be the true valuation of operator n 's desired resources at each BS m and $c'_{n,e}$ be the valuation of each inter-BS link e . Each operator's valuation is private information known to itself only. The utility of operator n is:

$$u_n(w_{n,m}, c_{n,e}) = \left(\sum_{m \in M} w'_{n,m} x_{n,m} + \sum_{e \in E} c'_{n,e} y_{n,e} \right) - p_n.$$

Following the convention in algorithmic game theory, operators are assumed to be selfish but rational. They are interested in maximizing their own utility and may not report their true valuations, i.e., $w_{n,m} \neq w'_{n,m}$ and $c_{n,e} \neq c'_{n,e}$, if doing so leads to a higher utility. The auctioneer instead wishes to maximize the aggregate social "happiness". Towards that goal, it is important for the auctioneer to elicit truthful bids from operators.

Definition 1. (Truthful action): A C-RAN auction is *truthful* if for any operator n , reporting the true node and link valuations maximizes its utility, regardless of other operators' bids. That is, for all $w_{n,m} \neq w'_{n,m}$ and $c_{n,m} \neq c'_{n,m}$, the following is always true: $u_n(w'_{n,m}, c'_{n,e}) \geq u_n(w_{n,m}, c_{n,e})$.

Definition 2. (Social welfare): The social welfare in the C-RAN auction is the sum of the aggregate operators' utility $\sum_{n \in [N]} (\sum_{m \in M} w'_{n,m} x_{n,m} + \sum_{e \in E} c'_{n,e} y_{n,e} - p_n)$ and the C-RAN's revenue $\sum_{n \in [N]} p_n$. Since Payments between C-RAN and operators cancel themselves, the social welfare is equal to $\sum_{n \in [N]} (\sum_{m \in M} w'_{n,m} x_{n,m} + \sum_{e \in E} c'_{n,e} y_{n,e})$.

4. C-RAN auction: point-to-point front-haul

We first consider resource allocation in the C-RAN with a point-to-point front-haul. We formulate the allocation problem into an integer linear program (Section 4.1). An exact algorithm based on dynamic programming is designed (Section 4.2), and an approximation scheme (Section 4.3) utilizes the exact algorithm on a well-structured solution subspace to return $(1-\epsilon)$ -optimal social welfare. Finally, the approximation scheme is transformed into a truthful MIR auction (Section 4.4).

4.1. Social welfare maximization for C-RAN with point-to-point front-haul

Under truthful bidding, the social welfare maximization problem in the C-RAN resource auction with a point-to-point front-haul can be formulated into the following integer linear program (ILP):

$$\text{Maximize } \sum_{n \in [N]} \left(\sum_{m \in M} w_{n,m} x_{n,m} + \sum_{e \in E} c_{n,e} y_{n,e} \right) \quad (1)$$

Subject To:

Input: an integer k , a C-RAN graph $G = (\mathcal{M}, \mathcal{E})$, operators' bids
Output: An optimal allocation S^* for ILP (1)

- 1: Cut a slice of G such that the number of nodes inside it is less than or equal to $2k$;
- 2: Let G_o denote subgraph induced by nodes inside the slice. Let set B_o include the boundary nodes of G_o ;
- 3: $\mathcal{M}' = \mathcal{M} \setminus G_o$; $\Lambda = \emptyset$;
- 4: **do**
- 5: Merge one neighbour node $m_n \in \mathcal{M}'$ into G_o , such that $|B_n| = 2k$. G_n and B_n are the new graph and the boundary set respectively;
- 6: $m_c = B_o \setminus B_n$; $\Lambda' = \emptyset$;
- 7: **for all** Allocation A for nodes in B_n ; **do**
- 8: Compute the allocation A' for G_n that agrees with A on B_n and maximizes the social welfare on G_n ; Save A' into Λ' if A' satisfies constraints (1a) and (1b);
- 9: **end for**
- 10: $\Lambda = \Lambda'$;
- 11: $\mathcal{M}' = \mathcal{M}' \setminus m_n$; $G_o = G_n$; $B_o = B_n$;
- 12: **while** $\mathcal{M}' \neq \emptyset$
- 13: $S^* = \arg \max_{S \in \Lambda} V(S)$;
- 14: **Return** S^*

Algorithm 1. An exact algorithm for C-RAN social welfare maximization (ILP (1)).

$$\sum_{n \in [N]} r_{n,m} x_{n,m} \leq R_m, \quad \forall m \in \mathcal{M} \quad (1a)$$

$$y_{n,e} \leq x_{n,m}, \quad \forall n \in [N], \forall m \in e, \forall e \in \mathcal{E} \quad (1b)$$

$$x_{n,m} \in \{0, 1\}, \quad \forall n \in [N], \forall m \in \mathcal{M} \quad (1c)$$

$$y_{n,e} \in \{0, 1\}, \quad \forall n \in [N], \forall e \in \mathcal{E} \quad (1d)$$

Constraint (1a) is the channel capacity constraint at each BS. Constraint (1b) guarantees that a link between two BSs is assigned to an operator only when the cloud allocates spectrum resources in both BSs to that operator. Constraints (1c) and (1d) model binary decisions.

Theorem 1. *The C-RAN social welfare maximization problem in ILP (1) is NP-hard, even if the number of BSs or the number of operators is constant.*

Proof. If the input C-RAN system has only one base station, then the social welfare maximization problem defined in ILP (1) degrades into the classic knapsack problem [11] that is known to be NP-hard.

If the number of operators (M) is a constant instead, the problem is also NP-hard. We prove this by reducing ILP (1) to the problem of maximum independent set in planar graphs, which is proven NP-Complete [11]. Next, we provide a sketch of the proof. Given a planar graph, we construct an instance of ILP (1) with five operators, where the first operator has very small valuations on links but large valuations on nodes, and the other four operators each has small valuations on nodes but extremely large valuations on links, such that an optimal solution must assign all the links to at least one of the other four operators. We then set the capacity constraint on each node in a way such that if the first operator wins the bids at two adjacent nodes, any one of the other four operators cannot gain the profit of that link. In an optimal solution of the constructed instance, the nodes with resources allocated to the first operator must form a maximum independent set of the planar graph. \square

The number of mobile operators (N) in a given C-RAN is usually no more than 5 in most regions in the world [33], but the number of BSs may vary widely. Given Theorem 1, it is unlikely to find an efficient algorithm that can compute the optimal allocation for large C-RAN systems.

4.2. An exact algorithm for C-RAN resource allocation

We now design an exact algorithm that always returns an optimal allocation in a given solution space, with a running time exponential in the number of BS layers. The algorithm adopts the classic dynamic programming approach to solve ILP (1). Note that there are direct links only between BSs in neighbouring cells, hence the C-RAN graph $G = (\mathcal{M}, \mathcal{E})$ is a k -outerplanar graph (planar graph with k “layers” of BS cells) as defined below.

Definition 3. (k -outerplanar graph): An outerplanar graph has a crossing free embedding in the plane such that all the vertices belong to the unbounded face of the embedding. A k -outerplanar graph has a planar embedding, and, deleting the vertices on the outer face results in a $(k - 1)$ -outerplanar graph. Note that a 1-outerplanar graph is an outerplanar graph.

The basic idea of the exact algorithm is to first build a set Λ of feasible allocations for a few BSs, and then gradually expand the set to all BSs, while keeping the optimal allocation on the already-examined BSs included in the set.

We first consider a set G' of BSs located in a continuous area, and let Λ include all possible allocations for these BSs. Each time we append one more BS to G' . The key observation is that for a fixed resource allocation of the “boundary” BSs of G' , i.e., BSs that are adjacent to some BS not in G' , the allocation of inner BSs will not affect future allocations of BSs not in G' . Therefore, we keep Λ containing all possible

allocations for the boundary BSs, and for each of them, we are able to fix the optimal resource allocation for the inner BSs. The process is repeated until G' contains all BSs. The most time consuming step is the enumeration of all possible allocations of boundary BSs. Therefore, we try to keep the boundary of G' small during the expansion of G' . Because the entire C-RAN is a k -outerplanar graph, we are able to expand G' to include all BSs while maintaining at most $2k$ BSs in the boundary of G' . The detailed algorithm is shown in Algorithm 1.

At line 5 of Algorithm 1, when we consider adding a neighbour BS into the set G_o , the new boundary has to include exactly $2k$ BSs. Under this condition, only one BS becomes the inner BS, and we can easily compute the best allocation (definition in line 8) of it and save that in the feasible solution set Λ . In line 8, the term *agree* is defined as follows: Let A be a partial allocation that allocates resources of BSs in $B \subseteq \mathcal{M}$ to operators. Then given a set $B' \subseteq B$ and two partial allocations A and A' , we say A agrees with A' on B' if $\forall m \in B', A(m) = A'(m)$, i.e., both allocations assign the resources in B' to the same operators. Note that when we compute A' , only $2k + 1$ nodes (in $m_c \cup B_n$) need to be considered. The best allocations for other BSs in G_n can be found in Λ as Λ contains the best allocation of G_o that agrees with every possible allocation of B_o on B_o . In line 16, $V(S)$ denotes the social welfare achieved by the allocation S .

Fig. 4 illustrates how Algorithm 1 conducts resource allocation. Here a 2-outerplanar graph models a C-RAN system with 11 BSs. **First**, we construct G_o as the set of BSs $\{2, 5, 3, 6\}$. Common BSs between G_o and the rest of G are boundary BSs $\{2, 5, 3, 6\}$, and they are inserted into set B_o . **First round**, $\{1, 5, 3, 6\} \rightarrow 2$: Merger a neighbour BS 1 into G_o . The new BS set is denoted as G_n and the new boundary BSs $\{1, 5, 3, 6\}$ are contained in set B_n . The common BS m_c between B_n and B_o is BS 2. BS 2 becomes an inner BS and therefore we can save the allocation of BS 2. Given an allocation of BSs in $\{1, 5, 3, 6\}$, we can compute the best allocation of BS 2 that maximizes the social welfare of the subnetwork induced by BSs $\{1, 5, 3, 6, 2\}$. If this particular allocation (for BSs $\{1, 5, 3, 6, 2\}$) satisfies constraints (1a) and (1b), it is saved into set Λ' . After checking every possible allocation of $\{1, 5, 3, 6\}$, we obtain a set Λ' that contains allocations of BSs in $\{1, 5, 3, 6, 2\}$. Then let $\Lambda = \Lambda', G_o = G_n$ and $B_o = B_n$. **Second round**, $\{4, 5, 3, 6\} \rightarrow \{1, 2\}$: BS 4 is added into G_n , which becomes $\{4, 5, 3, 6, 1, 2\}$. Boundary BSs are $\{4, 5, 3, 6\}$ and $m_c = 1$. Similarly, for every allocation of $\{4, 5, 3, 6\}$, there is a best allocation of $\{1, 2\}$ that maximizes the social welfare of G_n . Furthermore, for every possible allocation of $\{4, 5, 3, 6, 1\}$, we can find an allocation of $\{1, 5, 3, 6, 2\}$ in set Λ that agrees with it on $\{1, 5, 3, 6\}$, and then merge them to obtain an allocation of $\{4, 5, 3, 6, 1, 2\}$ and add that to Λ' . The process is repeated until all BSs are processed. At the end, Algorithm 1 outputs the allocation with the maximal social welfare.

Theorem 2. Upon termination, Algorithm 1 returns an optimal allocation for ILP (1).

Proof. An optimal allocation includes the resource allocation of all BSs. An allocation A with respect to a set of BSs $\mathcal{N}' \subseteq \mathcal{M}$ is a *candidate* if it agrees with an optimal solution on the node set \mathcal{N}' . We use the notation $A|_{\mathcal{N}'}$ to denote the part of allocation A on nodes \mathcal{N}' .

We prove the theorem by showing that at the end of each iteration

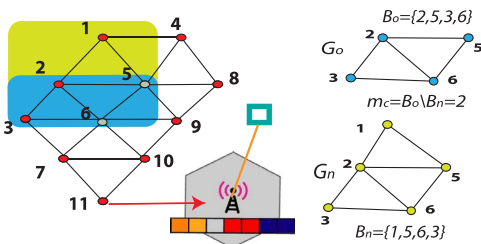


Fig. 4. Algorithm 1 applied to a 2-outerplanar graph. Each node represents a BS.

of the *do while* loop in Algorithm 1, the set Λ contains a candidate that agrees with the optimal allocation on G_o . When G_o grows to G and the *do while* loop terminates, one candidate in Λ is an optimal solution, and it will be selected as the return value at line 13.

After the first iteration, Λ contains all possible allocations for nodes in G_o , which must contain a candidate. Now assume at the beginning of the i th iteration of the *do while* loop, Λ contains a candidate. Let A^* denote the optimal solution, and $A^*|_{G_o}$ be the candidate. We show that after the execution of the current iteration, Λ still contains a candidate. In line 7, we enumerate all possible allocations A of B_n . Consider the case that A agrees with A^* . In line 8, we choose A' that maximizes the social welfare on nodes G_n and agrees with A , then the welfare of allocation $A' \cup A^*|(G - G_n)$ must be at least that of A^* , which implies $A' \cup A^*|(G - G_n)$ is also an optimal solution. Therefore, the set Λ also contains a candidate. \square

Theorem 3. The computation complexity of Algorithm 1 is $O\left((M - 2k) \binom{N}{\lfloor N/2 \rfloor}^{2k+1}\right)$.

Proof. Lines 1 and 2 can be executed in $O(1)$ steps. Line 3 deletes $2k$ BSs and initializes set Λ , which also takes constant time. Lines 5 to 11 are the body of the *do while* loop and will be executed $M - 2k$ times, since the size of \mathcal{M} is $M - 2k$ at the beginning and its size is decremented by one at line 11. During each iteration of the *do while* loop, running time of line 5 and line 6 is $O(1)$. Lines 7 to 9 are a *for* loop that processes each possible allocation for BSs in B_n . There are $2k$ BSs inside B_n , and each BS's resource can be shared among N operators. Hence, the total number of possible allocations is $(2^N)^{2k}$, where 2^N is the number of allocations for one BS. Note that all the bids $w_{n,m}$ and $c_{n,e}$, $\forall n, m, e$, are non-negative, the optimal social welfare can always be achieved with each node choosing a maximal allocation. Hence, we only need to consider all the maximal allocations for each BS. It can be proven that the number of different maximal allocations for one BS is no more than $\binom{N}{\lfloor N/2 \rfloor}$ [20].

At line 8, the number of possible allocations that agree with A on B_n is $\binom{N}{\lfloor N/2 \rfloor}$, as only m_c needs to be considered here. The allocation for other BSs can be found in Λ within $O(1)$ steps. Then finding the one with maximal social welfare takes $O\left(\binom{N}{\lfloor N/2 \rfloor}\right)$ steps. Checking the constants can be finished within $O(1)$ steps. In summary, the number of steps to execute the *for* loop is $\binom{N}{\lfloor N/2 \rfloor}^{2k} \left(O\left(\binom{N}{\lfloor N/2 \rfloor}\right) + O(1)\right)$. The running time of line 10 and line 11 is $O(1)$. Therefore, the running time of the entire loop is $(M - 2K) \left(\binom{N}{\lfloor N/2 \rfloor}^{2k} \left(O\left(\binom{N}{\lfloor N/2 \rfloor}\right) + O(1)\right) + O(1)\right)$, or $O\left((M - 2k) \binom{N}{\lfloor N/2 \rfloor}^{2k+1}\right)$. Line 13 examines $\binom{N}{\lfloor N/2 \rfloor}^{2k}$ allocations and outputs the optimal one, and the running time is $\binom{N}{\lfloor N/2 \rfloor}^{2k}$. In summary, the computation complexity of Algorithm 1 is $O\left((M - 2k) \binom{N}{\lfloor N/2 \rfloor}^{2k+1}\right)$. \square

4.3. A fast approximation scheme for C-RAN resource allocation

Theorem 3 reveals that the running time of Algorithm 1 is exponential in the number of layers k of the C-RAN graph. In a C-RAN system, a cloud can support up to the order of 1,000 base stations [21]. That translates into more than 20 layers in the cellular topology. When $k > 6$, the computation time is not acceptable even if only a small number of operators participate in the auction, motivating the design of a *polynomial-time* approximation algorithm. Aiming at a truthful auction at the end, we restrict our attention to *Maximum-in-Range (MIR)* algorithms [22]. A MIR algorithm works on a subset of feasible solutions, and outputs a solution that maximizes the social welfare over the given

Input: $\epsilon > 0$, a C-RAN graph $G = (\mathcal{M}, \mathcal{E})$, operators' bids

Output: An allocation S^f for ILP (1)

- 1: Determine the layer for each node in Graph G , let layer K be the highest layer;
- 2: Generate $k = \lceil 2/\epsilon \rceil - 1$;
- 3: **for all** $i \in \{1, 2, \dots, k+1\}$ **do**
- 4: Let P_i be the set of nodes who are in level $(i, (k+1) + i, 2(k+1) + i, \dots)$ of G ;
- 5: Subgraph G^i is induced by $\mathcal{M} \setminus P_i$. Each component of G^i is at most a k -outerplanar graph;
- 6: Compute the allocation S^i for G^i by running Algorithm 1 with the input $(k, G^i, \text{operators' bids})$;
- 7: **end for**
- 8: $S^f = \arg \max_{S^i} V(S^i)$;
- 9: **Return** S^f .

Algorithm 2. An $(1-\epsilon)$ -approximation scheme for ILP (1).

subset. The algorithm itself has to be maximizing without approximation loss (important for truthfulness), the room for manipulation lies in the choice of the subset of feasible solutions to perform optimization over.

Our design of the approximation scheme applies a decomposition technique, which divides a given k -outerplanar graph into a series of k' -outerplanar graphs with $k' < k$, and then calculates the optimal allocation for each k' -outerplanar graph. The final output is the allocation with maximal social welfare among them. The possible allocations on those k' -outerplanar graphs form the feasible solution set we pre-commit to. If we choose k' as a small constant, the algorithm can run in polynomial time. We can achieve $(1 - \epsilon)$ -optimal social welfare with $\epsilon \rightarrow 0$ as $k' \rightarrow k$ and $k \rightarrow \infty$. We present the detailed approximation scheme in Algorithm 2.

At line 1 of Algorithm 2, we label each layer of BSs from the outside to the core, as illustrated in Fig. 1. The value of k is set at line 2 based on the value of ϵ . A for loop from line 3 to line 7 decomposes G into $k+1$ subgraphs that can be solved by Algorithm 1. Line 8 selects the allocation with the maximal social welfare.

Fig. 1 shows a C-RAN system with 3 layers. Assuming 5 operators participating in the C-RAN auction, Algorithm 1 takes more than $11 \cdot 10^7$ steps. Alternatively, Algorithm 2 can be applied to compute an allocation within $11 \cdot 10^3$ steps. The speedup is already $100 \times$ in such a tiny network. First, Algorithm 2 calculates the value of k for the approximation ratio $1 - \epsilon = 0.33$. We obtain $k = 2$ in this example. Then it decomposes the C-RAN graph in Fig. 1 into three subnetworks G^1 , G^2 and G^3 as shown in Fig. 5. Here each G^i has one or two components that are at most 2-outerplanar. Algorithm 1 is applied on each k' -outerplanar graph ($k' \in \{1, 2\}$). The allocation of G^2 is the union allocation of its two components. The one among the three allocations with the maximal social welfare is the final solution.

Theorem 4. Given an input C-RAN $G = (\mathcal{M}, \mathcal{E})$, Algorithm 2 achieves $(1 - \epsilon)$ -optimal social welfare as defined in ILP (1).

Proof. Let S and α be the optimal allocation and the optimal social welfare obtained by S for ILP (1), respectively. The social welfare comes from two parts: contribution from BSs and contribution from links. For any BS $m \in \mathcal{M}$, let α_m be the contribution of m to the social welfare induced by S . For any link $e \in \mathcal{E}$, let α_e be the contribution of e to the social welfare induced by S . The optimal social welfare is $\alpha = \sum_{m \in \mathcal{M}} \alpha_m + \sum_{e \in \mathcal{E}} \alpha_e$.

For any P_i (line 4), let β_i be the partial social welfare of S when we consider only the contribution from BSs in P_i and links with at least one point in P_i , then $\beta_i = \sum_{m \in P_i} \alpha_m + \sum_{e \in \mathcal{E} \cap P_i \neq \emptyset} \alpha_e$.

If we add all partial social welfare β_i together, the sum of them is at most two times the optimal social welfare ($\sum_{i=1}^{k+1} \beta_i \leq 2\alpha$), as each BS in $\sum_{i=1}^{k+1} \beta_i$ is counted once and each link is counted at most twice. In lines 6 of Algorithm 2, the algorithm that optimizes the social welfare on the network induced by $\mathcal{M} \setminus P_i$ must return welfare of at least $\alpha - \beta_i$. In line 8, the allocation with the largest social welfare among the solutions for network $\mathcal{M} \setminus P_i$ is outputted, and the corresponding social welfare is at least:

$$\begin{aligned} \frac{1}{k+1} \sum_{i=1}^{k+1} (\alpha - \beta_i) &\geq \alpha - \frac{1}{k+1} \sum_{i=1}^{k+1} \beta_i \\ &\geq \alpha - \frac{2\alpha}{k+1} \geq \alpha - \epsilon\alpha \geq \alpha(1 - \epsilon). \end{aligned} \quad (2)$$

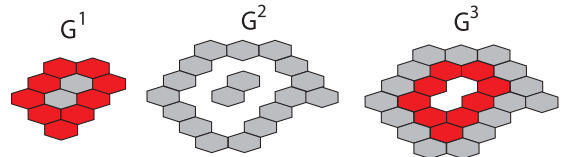


Fig. 5. Decomposition in Algorithm 2: an illustration using the C-RAN in Fig. 1.

Input: $\epsilon > 0$, a C-RAN graph $G = (\mathcal{M}, \mathcal{E})$, operators' bids

Output: An allocation S^f for ILP (1) and payment p_n

- 1: Run Algorithm 2 with the input $(\epsilon, G, \text{operators' bids})$, the output is S^f ;
- 2: Compute the payment for each winning operator n : $p_n = V(S_{-n}^f) - (V(S^f) - v_n(s_n^f))$;
- 3: **Return** the allocation S^f ;
- 4: **Return** the payment p_n for each winning operator n .

Algorithm 3. A truthful auction mechanism for C-RAN with point-to-point front-haul.

□

Theorem 5. The running time of Algorithm 2 is

$$O\left(M^2 \binom{N}{\lfloor N/2 \rfloor}^{\frac{4}{\epsilon}-1}\right), \text{ and is polynomial to } M \text{ with } N \text{ being a constant.}$$

Proof. Line 1 takes M steps to determine the layer number of each BS. Line 2 can be done in one step. The body of the *for* loop is iterated $k + 1$ times. Within the loop body, lines 4–5 can be done in $O(1)$ steps. Because each component has at most k layers, the running time of line 6 is $O\left(\lceil \frac{k}{\epsilon} \rceil (M - 2k) \binom{N}{\lfloor N/2 \rfloor}^{2k+1}\right)$. Line 9 takes one step and line 8 can be done in $k + 1$ steps. In summary, the running time of Algorithm 2 is $O\left((k + 1) \lceil \frac{k}{\epsilon} \rceil (M - 2k) \binom{N}{\lfloor N/2 \rfloor}^{2k+1}\right)$, which is the same as $O\left(M^2 \binom{N}{\lfloor N/2 \rfloor}^{\frac{4}{\epsilon}-1}\right)$. □

4.4. A truthful auction for C-RAN with point-to-point front-haul

We now transfer Algorithm 2 into a truthful auction, by tailoring a VCG-type payment scheme.

Theorem 6. Algorithm 2 is an MIR algorithm for the social welfare maximization problem in (1).

Proof. Recall that an MIR algorithm fixes the solution range, and returns a solution from the range that achieves the highest social welfare. We construct the solution range τ before the auction begins.

Let τ be the set of all feasible solutions for ILP (1) on G^i , $1 \leq i \leq k + 1$, where G^i is a subnetwork induced by BSs in $\mathcal{N} \setminus P_i$. Note that solutions in set τ are also feasible solutions to ILP (1) on the original C-RAN graph G . Lines 6 in Algorithm 2 compute the optimal allocation S^i for G^i , and then select the allocation S^f with the maximal social welfare among all S^i in line 8. It is clear that S^f also maximizes the social welfare over set τ .

In summary, Algorithm 2 is an MIR algorithm that achieves the maximal social welfare among all the solutions in the solution range τ that the algorithm pre-commits to. □

Next, in order to design a truthful auction, we utilize an important property of MIR algorithms: every MIR algorithm that works in concert with the VCG-type payments induces a deterministic truthful mechanism [22]. As a result, the payment can be expressed as the following:

$$p_n = V(S_{-n}^f) - (V(S^f) - v_n(s_n^f)). \quad (3)$$

Here p_n is the payment of each operator n . S_{-n}^f is the allocation output by Algorithm 2 when we set operator n 's bidding price to 0 on each node and each link. Therefore, $V(S_{-n}^f)$ is the social welfare when operator n is excluded from the auction. S^f is the solution returned by Algorithm 2 when every operator participates in the auction, and $V(S^f)$ is the social welfare of the solution S^f . s_n^f is the allocation for operator n , obtained from the entire allocation S^f . $V(S^f) - v_n(s_n^f)$ is the total social welfare except operator n .

Theorem 7. Algorithm 2 combined with the payment rule in (3) is a truthful auction.

Proof. An MIR allocation combined with a VCG-type payment rule belongs to the family of VCG mechanisms [22], rendering a truthful auction. It is well known that VCG mechanisms are truthful [13]. A mechanism belongs to the VCG family if it maximizes the social welfare on a finite set of allowed output and the payment is calculated according to VCG formula [22]. We can observe that an MIR allocation algorithm with a VCG-type payment is a VCG mechanism where the set of allowable output is the solution range of its algorithm. □

The C-RAN auction mechanism is summarized in [Algorithm 3](#).

Theorem 8. *Algorithm 3 is a truthful auction mechanism for the social welfare maximization problem in (1). It runs in polynomial time and achieves $(1 - \epsilon)$ -optimal social welfare.*

Proof. The theorem follows from [Theorems 4, 5 and 7](#). \square

4.5. Further improving social welfare

[Algorithm 2](#) ignores several layers of BSs due to network decomposition, which is an apparent waste of RRH resources. We can pursue a higher social welfare in practice by introducing a post-processing step to [Algorithm 2](#), to allocate resources at the ignored BSs and their adjacent links. Note that all the dropped layers form a 1-outerplanar graph, we can call [Algorithm 1](#) to efficiently compute the optimal resource allocation for such 1-outerplanar graphs. Specifically, [Algorithm 4](#) is inserted between line 6 and line 7 in [Algorithm 2](#).

While [Algorithm 2](#) + [Algorithm 4](#) achieves higher social welfare, the new allocation does not come from the solution range τ , and hence the improved algorithm is not an MIR algorithm on τ . Next, we construct a new solution range for [Algorithm 2](#) + [Algorithm 4](#) and prove its MIR property in [Theorem 9](#).

Theorem 9. *Algorithm 2 + Algorithm 4 is an MIR algorithm.*

Proof. First, let a *joint allocation* be the concatenation of feasible allocations on graphs G^i and $G^{P_i}, 1 \leq i \leq k + 1$. Note that a joint allocation is a feasible allocation for the original graph G . Let τ' denote the set that contains all the joint allocations.

At line 3 in [Algorithm 4](#), we can observe that S^i is the optimal allocation for graph G^i and S^{P_i} is the optimal allocation for graph G^{P_i} . Combining them together provides a joint allocation with the maximal social welfare for the graph $G^i \cup G^{P_i}$. Next, S^f is selected among all S^i , achieving the maximal social welfare among S^i and therefore among all the solutions in set τ' . If we fix τ' to be the solution range, then [Algorithm 2](#) + [Algorithm 4](#) is an MIR algorithm that returns an allocation with maximal social welfare over this solution range. \square

Theorem 10. *Algorithm 2 + Algorithm 4 coupled with the payment scheme in (3) is a truthful auction mechanism that runs in polynomial time and achieves $(1 - \epsilon)$ -optimal social welfare.*

Proof. The proof of truthfulness and the approximation guarantee are similar to the proof in [Theorems 4 and 7](#). The running time of the improved algorithm is still polynomial as the subgraph G^{P_i} includes less than $\lceil \frac{K}{k} \rceil$ outerplanar graphs, and the running time of the *for* loop is

$O\left(2^{\lceil \frac{K}{k} \rceil} (M - 2k) \binom{N}{\lfloor N/2 \rfloor}^{2K+1}\right)$. The overall complexity of the [Algorithm 2](#) + [Algorithm 4](#) is still

$$O\left(M^2 \binom{N}{\lfloor N/2 \rfloor}^{\frac{4}{\epsilon}-1}\right).$$

\square

5. C-RAN auction: daisy-chain front-haul

In this section, we study C-RAN resource allocation with a daisy-chain front-haul. We model the virtualized resource allocation problem for such C-RANs in [Section 5.1](#), and design a truthful auction mechanism in [Section 5.2](#).

5.1. Social welfare maximization for C-RAN with daisy-chain front-haul

Under truthful bidding, the social welfare maximization problem in the daisy chain front-haul model can be formulated into the following

- 1: Let G^{P_i} be the subgraph that is induced by nodes in P_i ;
- 2: Run [Algorithm 1](#) on the subgraph G^{P_i} , and output the solution S^{P_i} ;
- 3: $S^i = S^i \cup S^{P_i}$;

[Algorithm 4.](#) Improvement to [Algorithm 2](#).

integer linear program (ILP):

$$\text{Maximize } \sum_{n \in [N]} \left(\sum_{m \in M} w_{n,m} x_{n,m} + \sum_{e \in E} c_{n,e} y_{n,e} \right) \quad (4)$$

Subject To:

$$\sum_{n \in [N]} r_{n,m} x_{n,m} \leq R_m, \quad \forall m \in M \quad (4a)$$

$$\sum_{m \in g} \sum_{n \in [N]} r_{n,m} x_{n,m} \leq C_g, \quad \forall m \in g, \forall g \quad (4b)$$

$$y_{n,e} \leq x_{n,m}, \quad \forall n \in [N], \forall m \in e, \forall e \in E \quad (4c)$$

$$x_{n,m} \in \{0, 1\}, \quad \forall n \in [N], \forall m \in M \quad (4d)$$

$$y_{n,e} \in \{0, 1\}, \quad \forall n \in [N], \forall e \in E \quad (4e)$$

Constraints (4a), (4c), (4d) and (4e) are the same as constants (1a), (1b), (1c) and (1d). The capacity constraint of the front-haul is modelled in constraint (4b). Note that ILP (1) is a special case of ILP (4). Following Theorem 1, we know that ILP (4) is also NP-hard even if the number of operators or the number of BSs is constant.

5.2. Truthful auction for C-RAN with daisy-chain front-haul

A new exact algorithm for solving ILP (4) is shown in Algorithm 5, which extends from Algorithm 1. The difference is that, we can only fix the optimal allocation of an inner BS when all BSs sharing a common front-haul link with it have been included in G_n . As we expand the BS set from G_o to G_n , more and more transmission groups are entirely included in G_n . We define the newly included groups ($g \subseteq G_n$ and $g \not\subseteq G_o$) as *unprocessed* groups.

Next, we will use the 2-outerplanar graph in Fig. 4 to illustrate the idea of Algorithm 5. We assume that BSs are divided into two groups: $\{1, 4, 2, 5, 8\}$ and $\{3, 6, 9, 7, 10, 11\}$. First, we construct G_o to include a set of BSs $\{2, 5, 3, 6\}$. Boundary BSs are $\{2, 5, 3, 6\}$. **First round**, G_o takes over a neighbour BS 1. The new BS set is denoted as G_n and the new boundary BSs are $\{1, 5, 3, 6\}$. There doesn't exist any unprocessed group in G_n , so the algorithm continues to run. **Second round**, BS 4 is added into G_n , which becomes $\{4, 5, 3, 6, 1, 2\}$. Boundary BSs are $\{4, 5, 3, 6\}$. Again, the algorithm continues to run as there still doesn't exist any unprocessed group. **Third round**, BS 8 is included into G_n . Now $G_n = \{8, 5, 3, 6, 2, 1, 4\}$ and $B_n = \{8, 5, 3, 6\}$. BSs 2, 1 and 4 become inner BSs and therefore we can save the allocations for them. More specifically, given an allocation of BSs in $\{8, 5, 3, 6\}$, we can compute the best allocation of BSs $\{2, 1, 4\}$ that agrees with it and maximizes the social welfare of the subnetwork induced by BSs $\{8, 5, 3, 6, 2, 1, 4\}$. If this particular allocation (for BSs $\{8, 5, 3, 6, 2, 1, 4\}$) satisfies constraints (4a), (4b) and (4c), it is saved into set Λ' . After checking every possible allocation of $\{8, 5, 3, 6\}$, we obtain a set Λ' that contains allocations of BSs in $\{8, 5, 3, 6, 2, 1, 4\}$. Then let $\Lambda = \Lambda'$. The process is repeated until all BSs are processed.

Theorem 11. *The computation complexity of Algorithm 5 is $O\left(M \binom{N}{\lfloor N/2 \rfloor}^{2k+kl+1}\right)$.*

Proof. The *for* loop in Algorithm 5 is executed when there exist unprocessed groups. The boundary of the current set of BSs G_o is divided into two sides each with k BSs. For example, in Fig. 4, G_o 's boundary includes two sides $\{3, 6\}$ and $\{2, 5\}$. When we add a neighbour node to the current subgraph G_o , that node must be adjacent to one side of G_o 's boundary. Because the longest distance between two BSs in one group is l , there must exist unprocessed groups when kl BSs have been inserted into the first G_o . At this point, we can compute the allocations for $2k + kl$ BSs, and record the best allocation for the inner BSs that are in group g . The process is repeated at most M

```

1: if  $\exists$  unprocessed groups  $g \subseteq G_n$  then
2:    $\Lambda' = \emptyset$ ;
3:   for all Allocation  $A$  for BSs in  $(G_n \setminus g) \cup B_n$  do
4:     Compute the allocation  $A'$  for BSs in  $G_n$  that agrees with  $A$  on  $(G_n \setminus g) \cup B_n$  and maximizes the social welfare for  $G_n$ ;
5:     Save  $A'$  into set  $\Lambda'$ ;
6:   end for
7:    $\Lambda = \Lambda'$ ;
8: end if

```

Algorithm 5. An exact algorithm for ILP (4): Algorithm 1 with lines 6–10 replaced by the following.

2. Generate $k = \lceil 2l/\epsilon \rceil - 1$;
4. Let P_i be the set of nodes in level $(i, i + 1, \dots, i + l - 1); ((k + l) + i + 1, \dots, (k + l) + i + l - 1); (2(k + l) + i, 2(k + l) + i + 1, \dots, 2(k + l) + i + l - 1), \dots$ of G ;
6. Compute the allocation S^i for G^i by running Algorithm 5 with the input $(k, G^i, \text{operators' bids})$;

Algorithm 6. The $(1-\epsilon)$ -Approximation Scheme for ILP (4): Algorithm 2 with lines 2, 4 and 6 replaced by the following.

times. Therefore the running time of Algorithm 5 is $O\left(M \binom{N}{\lfloor N/2 \rfloor}^{2k+kl}\right)$ when $l \geq 1$. An extra 1 is added to the exponent to ensure correctness when $l = 0$. \square

Next, we design an approximation algorithm to solve ILP (4) (Algorithm 6). The algorithm differs from Algorithm 2 slightly, to ensure that the front-haul capacity constraint is satisfied during the decomposition. For instance, consider an input network G with eight layers. When $\epsilon = 0.8$ and $l = 2$, then $k = 4$. G is decomposed into five subnetworks:

$$G^1 = G \setminus 1 \setminus 2 \setminus 7 \setminus 8; G^2 = G \setminus 2 \setminus 3 \setminus 8; G^3 = G \setminus 3 \setminus 4; G^4 = G \setminus 4 \setminus 5; G^5 = G \setminus 5 \setminus 6.$$

Theorem 12. Algorithm 6 achieves $(1 - \epsilon)$ -optimal social welfare for ILP (4).

Proof. The analysis of the approximation guarantee is similar to that in Theorem 4. Recall that S and α are defined as the optimal allocation and the optimal social welfare for ILP (4). β_i is the partial social welfare from the contribution of BSs in P_i and from links with at least one point in P_i . When we add the $k + 1$ partial social welfare together, $\sum_{i=1}^{k+1} \beta_i \leq 2l\alpha$ because every BS is counted at most l times and every link is counted at most $2l$ times. As a result, the social welfare returned by the approximation algorithm is at least: $\left(1 - \frac{2l}{k+1}\right)\alpha \geq (1 - \epsilon)\alpha$. \square

We further combine Algorithm 6 with the VCG-style payment in (3), and a truthful auction is obtained. The workflow of the auction is similar to that in Algorithm 3.

Theorem 13. Combining Algorithm 6 with the VCG-style payment in (3) renders a truthful auction, which runs in polynomial time and achieves $(1 - \epsilon)$ -optimal social welfare for ILP (4).

Proof. If we fix a solution range τ that includes all the feasible solutions for ILP (4) on graph G^i , $1 \leq i \leq k + 1$, the approximation algorithm is an MIR algorithm that outputs an allocation with the maximal social welfare among the solution range. It can work with the payment rule in (3), for constituting a auction mechanism whose truthfulness is guaranteed by the property of MIR algorithms. The time complexity analysis is similar to that in Theorem 5. $(1 - \epsilon)$ -optimality is proved in Theorem 12. \square

Finally, implementing Algorithm 4 inside Algorithm 6 further improves the social welfare in practice. Note that, when we compute the allocation for graph G^{P_i} , the front-haul capacity constraints for graph G^{P_i} need to be updated according to the allocation for graph G^i . Algorithm 6 + Algorithm 4 is still an MIR algorithm that returns the best allocation among a pre-committed solution range τ . Here τ includes all the joint allocations. A joint allocation consists of one feasible solution on G^i and one corresponding solution on G^{P_i} under the revised front-haul capacity constraints. Hence, combining this MIR algorithm with VCG payments in (3) still renders a truthful auction.

6. Performance evaluations

To thoroughly examine the performance of our auctions in large-scale C-RANs, we carried out simulation studies driven by real world traces. We set the number of required resource blocks $r_{n, m}$ according to real world traffic loads [23]. As shown in Fig. 6a, the location of each BS is classified into two types: a business cell or a residential cell. For each cell, we generate the traffic load with the chosen peak hour according to the reported distribution [23], which is usually in the evening for a residential cell and during the day time for business cell. Figs. 6c and d show the traffic load at 10 A.M. and 10 P.M., respectively.

Operator n offers $w_{n, m}$ for the resources at BS m , which is proportional to the amount of resources $r_{n, m}$. However, the normalized valuation $w_{n, m}/r_{n, m}$ may vary for different operators and different BSs. For the utility $c_{n, e}$ of an inter-BS link e , we assume that it is proportional

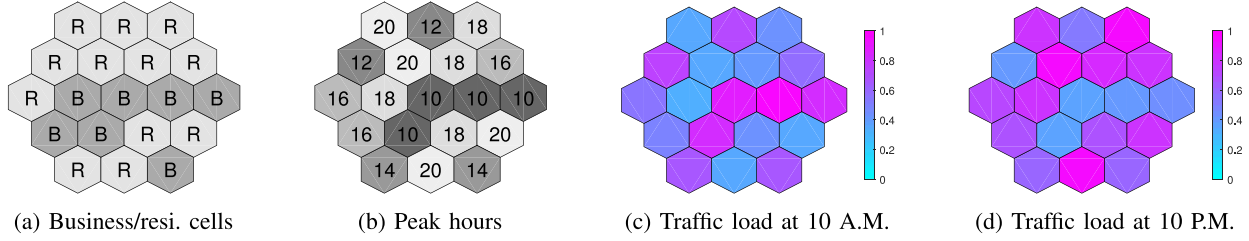
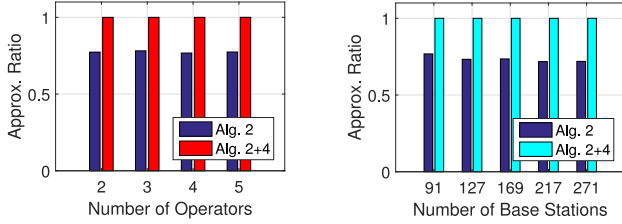
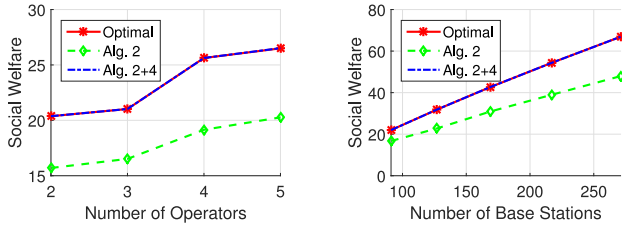


Fig. 6. Cellular traffic load distribution.



(a) Approximation Ratio under different numbers of operators. (b) Approximation Ratio under different numbers of BSs



(c) Social welfare under different number of operators (d) Social welfare under different number of BSs

Fig. 7. Performance of C-RAN auction under different number of operators and BSs.

to $r_{n,u} + r_{n,v}$, where u and v are the two end points of link e .

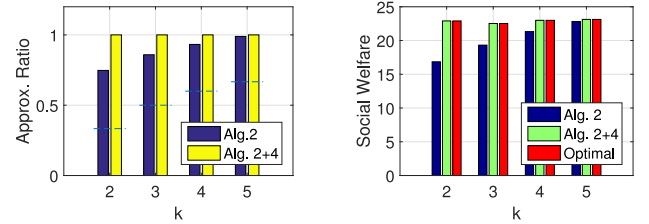
6.1. C-RAN with point-to-point front-haul

We study the approximation ratio of Algorithm 2 with and without the improvement of Algorithm 4, under different numbers of participating operators and base stations. The approximation ratios and overall social welfare are shown in Fig. 7a–d. We can see that, in all the tested scenarios, Algorithm 2 + Algorithm 4 achieves a social welfare very close to the optimum social welfare.

In Fig. 7a, there are 91 base stations that form a cellular network of 6 layers, and we set $k = 2$ for both Algorithm 2 and Algorithm 2 + Algorithm 4. We can see that the performance of Algorithm 2 is not affected by the number of operators.

In Fig. 7b, we fix the number of operators to 3 and vary the number of BSs from 91 (6 layers) to 271 (10 layers), with $k = 2$ in both algorithms. The approximation ratio of Algorithm 2 + Algorithm 4 remains very close to 1, whereas the approximation ratio of Algorithm 2 decreases slightly with small fluctuations as the number of BSs grows. This is because in Algorithm 2, we discard the resources in some layers of BSs. As the number of layers grows, an optimal solution is more likely to require a joint consideration of several base stations in adjacent layers, which is ignored in Algorithm 2. This explains the slight decrease of the approximation ratio. The fluctuations are caused by the rounding effect, as we drop $\lfloor \frac{k}{K} \rfloor$ layers for different K .

The overall social welfare obtained by each algorithm are illustrated in Fig. 7c and d. We can see that the social welfare grows as the number of BSs and the number of operators increase. This is because more BSs brings more resources for allocation, and more operators expands the allocation solution space.



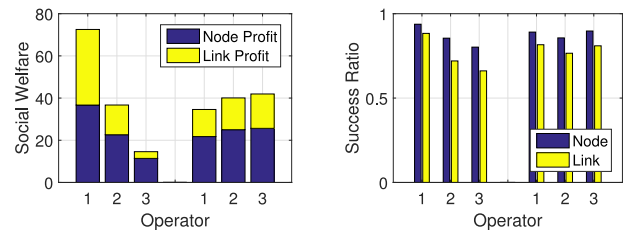
(a) Approximation ratio (b) Social welfare.

Fig. 8. Performance of C-RAN auction under different values of k .

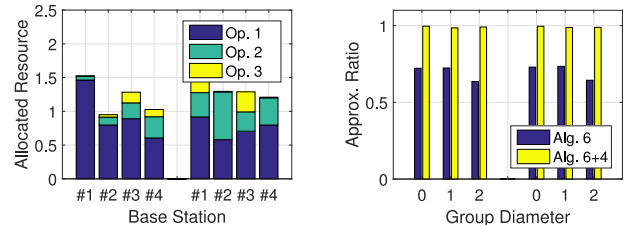
Fig. 8a and b show the approximation ratios and social welfare achieved by Algorithm 2 with and without the improvement of Algorithm 4. Here the number of BSs is 91, the number of operators is 3, and k vary from 2 to 5. The performance of Algorithm 2 becomes better as k grows, because more layers of BSs are jointly considered to find a good allocation. The guaranteed approximation ratios are marked with dashed lines. Note that the approximation ratios observed in trace-based simulations are much better than the theoretical ratio $1 - \frac{2}{k+1}$.

We further assume that the operators have different market shares, i.e., they have different numbers of subscribers and hence require different amount of resources. For example, the United States has four major telecom operators, Verizon, AT&T, Sprint and T-Mobile, with market shares of about 30%, 30%, 15% and 15%; in Canada, there are three operators, with market shares of 36%, 32% and 31% [33]. To test the impact of different market shares, we conduct two sets of simulations with market shares [50%, 30%, 20%] and [30%, 30%, 30%], respectively. The results are shown in Fig. 9a–d.

Fig. 9a–c show the impact of market share in point-to-point front-haul model when running Algorithm 2 + Algorithm 4. From Fig. 9a, we can see that the utility of each operator is proportional to its market



(a) Social welfare. (b) Bids winning ratio.



(c) Allocated resource. (d) Approximation Ratio.

Fig. 9. Impact of different market shares: [50%, 30%, 20%] (left) and [30%, 30%, 30%] (right).

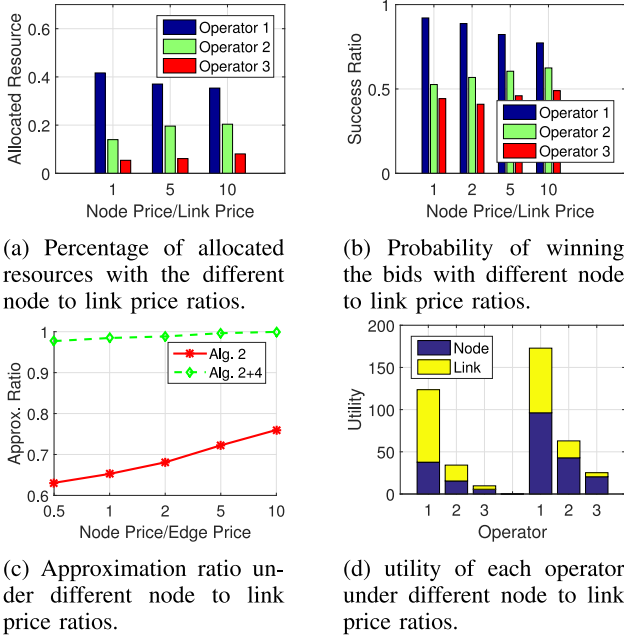


Fig. 10. Performance of C-RAN auction under different node to link price ratios.

share. Another interesting observation is on the composition of the utility. Larger the operator is, larger the utility that is from the inter-BS links is. The reason is that larger operator’s bid covers more BSs and links, and meanwhile, our solution assigns resources to large operator to fully exploit the utility of links. Fig. 9b shows the probability of winning its bid for each operator. We can see that our algorithms are more likely to assign resources to large operators rather than small ones, because large operators are more likely to enjoy the links. Fig. 9c shows the resource allocation on some BSs, verifying the fact that larger operators are preferred in the resource allocation. Fig. 9d shows the approximation ratio for C-RAN with daisy chain front-haul. The diameter of the transmission group l varies from 0 to 2. The approximation ratio of the improved algorithm (Algorithm 6 + Algorithm 4) is very close to 1 in both types of market shares.

The ratio of average node price to link price is a key factor that affects the resource allocation. We scale node prices with different factors to test how our algorithms perform in different scenarios. The results are shown in Fig. 10a–d.

Fig. 10a shows the percentages of resources allocated to each operator. As link utility decreases, resources allocated to each operator become more proportional to its market share ([50%, 30%, 20%]). This effect is verified by the operator’s probability of winning the bids, which is shown in Fig. 10b.

Fig. 10c shows the approximation ratios of Algorithm 2 with and without the improvement of Algorithm 4. Both algorithms perform better with larger node prices. This is because if the utility of nodes is larger, the interplay between adjacent BSs becomes less important, which reduces the potential loss of our algorithms. Our algorithms can then find the optimal allocation for each subnetwork.

Fig. 10d shows the utility of each operator with node to link price ratio set to 2 (left) and 5 (right). We see that the node contributes more utility and the utility of each operator tends to be proportional to their market share.

6.2. C-RAN with daisy chain front-haul

We tested algorithms proposed for C-RAN with daisy chain front-haul under same setting as in the previous section, and obtained similar observations. Hence we omitted some figures here. Additionally, we conduct a set of simulations that vary the maximum diameter l of the

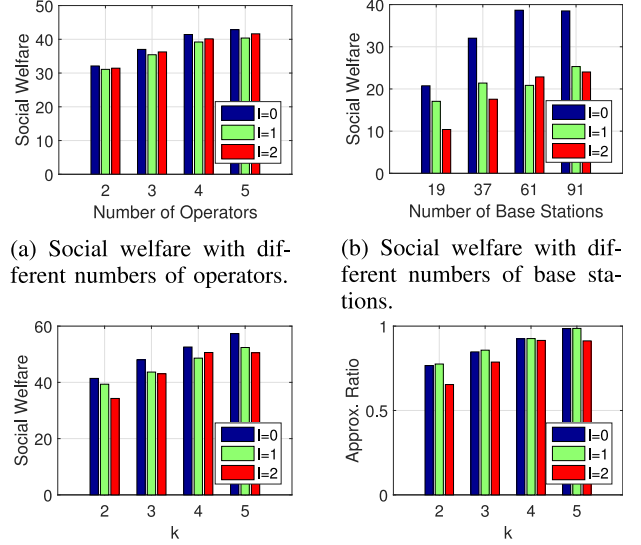


Fig. 11. Performance of C-RAN auction with daisy chain front-haul.

transmission group from 0 to 2. For the case of $l = 0$, each group contains only one BS, and we assume that its optical fibre has sufficiently large capacity. We test the performance of Algorithm 6 + Algorithm 4 (Fig. 11a and b) and Alg. 6 (Fig. 11c and d), with different numbers of operators, different numbers of BSs and different values of k . The value of k in Fig. 11a and b is set to 2 and the value of G_g is a random number that is less than the largest transmission rate of group g . We can see that the social welfare becomes larger with more operators or more BSs. For larger l , the optical fibres are shared by more BSs, which implies less available resources for each BS. This explains the decrease of social welfare as l increases.

A key factor affecting social welfare is the capacity of optical links shared by BSs in the same group. We conduct another set of simulations where the group link capacity is proportional to the largest transmission rate of group g . The social welfare under different group link capacities is shown in Fig. 12a. We can see that the social welfare almost grows linearly as the group link capacities grow.

Fig. 12b shows the resource utilization ratio at a business cell (BS 1) and a residential cell (BS 2). We can see that they have different traffic load patterns and the maximum usage ratio is about 90% at their peak hours.

7. Conclusion

As cellular infrastructure ownership is separated from cellular service provisioning, mobile operators now need to lease resources from

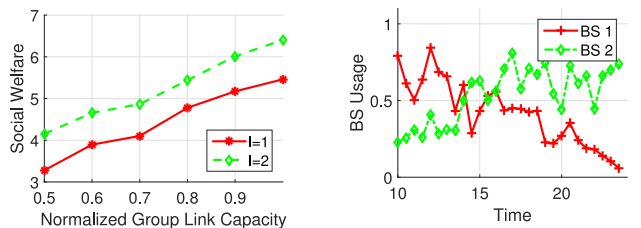


Fig. 12. Performance of C-RAN auction under different settings.

the C-RAN to serve its customers. The underlying algorithmic structure of such C-RAN resource auction is unique in that each operator's bid can be specified as a capacitated sub-network of the C-RAN, and the auctioneer needs to solve a sub-network packing problem that is computationally very hard. This work draws the community's attention to the emerging C-RAN resource sharing problem, and proposes a first solution based on MIR auction theory. The proposed auction is truthful, polynomial-time executable, guarantees $(1 - \epsilon)$ -optimal C-RAN-wide social welfare, and is evaluated through simulation studies. Note that the time complexity of our mechanism grows quickly with the increase of the number of mobile operators (N), and is exponential to $\frac{4}{\epsilon} - 1$. When there exists a high precision requirement in social welfare optimization, it may not be practical to apply our mechanism to a large number of mobile operators. A natural direction for future research is to study fast C-RAN resource allocation algorithms for large scale input. It will also be interesting to investigate the online C-RAN resource sharing problem.

References

- [1] Crown Castle, <http://www.crowncastle.com/wireless-carriers/towers.aspx>.
- [2] A late base station company, <http://www.infzm.com/content/101031>.
- [3] National base station company, <http://baike.baidu.com/view/13059527.htm>.
- [4] I. Abraham, M. Babaioff, S. Dughmi, T. Roughgarden, Combinatorial auctions with restricted complements, *Proc. of ACM EC*, (2012).
- [5] Alcatel-Lucent, LightRadio network: evolve your wireless broadband network, <http://www.alcatel-lucent.com/solutions/lightradio>.
- [6] B.S. Baker, Approximation algorithms for np-complete problems on planar graphs, *J. ACM (JACM)* 41 (1) (1994) 153–180.
- [7] S. Beaudin, F. Gao, D. Tholl, M. Parvan, J.B. DeForge, Agile remote radio head, 2012, US Patent 8,204,544.
- [8] S. Bhaumik, S.P. Chandrabose, M.K. Jataproul, G. Kumar, A. Muralidhar, P. Polakos, V. Srinivasan, T. Woo, Cloudiq: a framework for processing base stations in a data centre, *Proc. of ACM MobiCom*, (2012).
- [9] P. Chanclou, A. Pizzinat, F. Le Clech, T. Reedeker, Y. Lagadec, F. Saliou, B. Le Guyader, L. Guillo, Q. Deniel, S. Gosselin, et al., Optical fibre solution for mobile fronthaul to achieve cloud radio access network, *Proc. of Future Network Summit*, (2013).
- [10] S. Gandhi, C. Buragohain, L. Cao, H. Zheng, S. Suri, Towards real-time dynamic spectrum auctions, *Comput. Netw.* 52 (4) (2008) 879–897.
- [11] M.R. Garey, D.S. Johnson, *Computer and Intractability: A Guide to the Theory of NP-Completeness*, Elsevier, 1979.
- [12] A. Gopinathan, Z. Li, Strategyproof auctions for balancing social welfare and fairness in secondary spectrum markets, *IEEE INFOCOM*, (2011).
- [13] T. Groves, Incentives in teams, *Econometrica* 41 (4) (1973) 617–631.
- [14] S. Gu, Z. Li, C. Wu, H. Zhang, Virtualized resource sharing in cloud radio access networks through truthful mechanisms, *IEEE Trans. Commun.* PP (99) (2016). 1–1
- [15] J. Huang, R. Duan, C. Cui, X. Jiang, L. Li, et al., Recent progress on c-ran centralization and cloudification, (2014).
- [16] Telesystem Innovations, LTE in a Nutshell, White Paper, (2010). <https://home.zhaw.ch/kunr/NTM1/literatur/LTE%20in%20a%20Nutshell%20-%20Physical%20Layer.pdf>.
- [17] R. Irmer, H. Droste, P. Marsch, M. Grieger, G. Fettweis, S. Brueck, H.-P. Mayer, L. Thiele, V. Jungnickel, Coordinated multipoint: concepts, performance, and field trial results, *IEEE Commun. Mag.* 49 (2) (2011) 102–111.
- [18] V. Jungnickel, K. Manolakis, W. Zirwas, B. Panzner, V. Braun, M. Lossow, M. Sternad, R. Apelfrjd, T. Svensson, The role of small cells, coordinated multipoint, and massive mimo in 5g, *IEEE Commun. Mag.* 52 (5) (2014) 44–51.
- [19] C. B. N. Limited, Backhauling X2, <http://cbln.com/sites/all/files/userfiles/files/Backhauling-X2.pdf>.
- [20] MATHEMATICS, Find maximal number of subsets of the set U such that no one is a subset of another, <http://goo.gl/XITxn9>.
- [21] C. Mobile, C-ran: the road towards green ran, (2013). White Paper, version 3.0
- [22] N. Nisan, A. Ronen, Computationally feasible vcg mechanisms. *J. Artif. Intell. Res. (JAIR)* 29 (2007) 19–47.
- [23] C. Peng, S. Lee, S. Lu, H. Luo, H. Li, Traffic-driven power saving in operational 3g cellular networks, *Proc. of ACM MobiCom*, (2011).
- [24] D. Pompili, A. Hajisami, T.X. Tran, Elastic resource utilization framework for high capacity and energy efficiency in cloud ran, *IEEE Commun. Mag.* 54 (1) (2016) 26–32.
- [25] M. Ritter, Why C-RAN front-haul is a big challenge to existing network infrastructure technologies, <http://goo.gl/ULxltj>.
- [26] W. Shi, L. Zhang, C. Wu, Z. Li, F. Lau, An online auction framework for dynamic resource provisioning in cloud computing, *Proc. of ACM SIGMETRICS*, (2014).
- [27] D. Sun, G. Chang, C. Wang, Y. Xiong, X. Wang, Efficient nash equilibrium based cloud resource allocation by using a continuous double auction, *Proc. of IEEE ICCDA*, (2010).
- [28] K. Sundaresan, M.Y. Arslan, S. Singh, S. Rangarajan, S.V. Krishnamurthy, Fluidnet: a flexible cloud-based radio access network for small cells, *Proc. of ACM MobiCom*, (2013).
- [29] J. Tang, W.P. Tay, T.Q. Quek, Cross-layer resource allocation in cloud radio access network, *IEEE GlobalSIP*, (2014).
- [30] Wikipedia, 5G, <http://en.wikipedia.org/wiki/5G>.
- [31] Wikipedia, Base station subsystem, http://en.wikipedia.org/wiki/Base_station_subsystem.
- [32] Wikipedia, C-RAN, <http://en.wikipedia.org/wiki/C-RAN>.
- [33] Wikipedia, List of mobile network operators, http://en.wikipedia.org/wiki/List_of_mobile_network_operators.
- [34] S. Zaman, D. Grosu, Combinatorial auction-based allocation of virtual machine instances in clouds, *J Parallel Distrib Comput* 73 (4) (2013) 495–508.
- [35] L. Zhang, Z. Li, C. Wu, Dynamic resource provisioning in cloud computing: randomized auction approach, *Proc. of IEEE INFOCOM*, (2014).
- [36] Q. Zhang, Q. Zhu, R. Boutaba, Dynamic resource allocation for spot markets in cloud computing environments, *Proc. of IEEE UCC*, (2011).
- [37] X. Zhang, Z. Huang, C. Wu, Z. Li, F.C. Lau, Online auctions in iaas clouds: Welfare and profit maximization with server costs, *Proc. of ACM SIGMETRICS*, (2015).
- [38] K. Zhu, E. Hossain, Virtualization of 5g cellular networks as a hierarchical combinatorial auction, *IEEE Trans. Mob. Comput.* 15 (10) (2015) 2640–2654.
- [39] Y. Zhu, Z. Zhang, Z. Marzi, C. Nelson, U. Madhoo, B.Y. Zhao, H. Zheng, Demystifying 60ghz outdoor picocells, *Proc. of ACM MobiCom*, (2014).
- [40] Z. Zhu, P. Gupta, Q. Wang, S. Kalyanaraman, Y. Lin, H. Franke, S. Sarangi, Virtual base station pool: towards a wireless network cloud for radio access networks, *Proc. of ACM Computing Frontiers*, (2011).